Methyl Radical Addition to C═S Double Bonds: Kinetic versus Thermodynamic Preferences

Michelle L. Coote,* Geoffrey P. F. Wood, and Leo Radom*

Research School of Chemistry, Australian National University, Canberra, ACT 0200, Australia

Received: August 15, 2002; In Final Form: October 21, 2002

Barriers and enthalpies for methyl radical addition to both the C- and S-centers of CH_2═S, CH_3CH═S, and $(CH_3)_2C$═S, and for the methyl-transfer reactions that interconvert the S-centered and C-centered radical products have been calculated via a variety of high-level ab initio molecular orbital procedures, including variants of the CBS, G3, G3-RAD, and W1 methods. An extensive assessment of the performance of the various theoretical procedures has been carried out. One of the important conclusions of this assessment is that the B3-LYP geometries, prescribed for several of these high-level composite methods, greatly overestimate the forming bond length in the addition transition structures, leading to a significant underestimation of the reaction barriers. The addition reactions are found to be highly exothermic and have relatively low barriers that are increased somewhat on methyl substitution. The reactions are also contra-thermodynamic—that is, despite a clear thermodynamic preference for the S-centered radical product, the barriers for the production of the C-centered radical via addition to S are lower. Interconversion of the C-centered and S-centered radical products via a methyl-transfer reaction is a high-energy process.

1. Introduction

The addition of carbon-centered radicals to C═S double bonds is important in atmospheric chemistry, combustion chemistry, and in a number of chemical syntheses, of which the reversible-addition-fragmentation-transfer ("RAFT") process for control of molecular weight and architecture in free-radical polymerization is a notable recent example.[1−3] However, despite its importance, comparatively few theoretical studies have been performed on radical addition to the C═S double bond and much is yet to be learned concerning the fundamental aspects of this class of reactions.

There has been recent speculation concerning whether the addition to C═S double bonds occurs predominantly at the carbon or at the sulfur centers. Macrae and Carmichael[4] used density functional theory to show that the C-adducts of a range of thiocarbonyl compounds are significantly more stable than the corresponding S-adducts. However, in contrast, they also showed that ESR signals for radicals produced by muonium (a light isotope of hydrogen) addition to C═S bonds in solution correspond to those of the (less-stable) S-adduct. They speculated that this apparent contradiction may be the result of a kinetic preference for addition to the sulfur. This idea is, to some extent, supported by earlier theoretical work by Chiu et al.[5] In the course of a general study of C_2H_5S isomers using G2 theory,[6] they calculated the barriers and enthalpies for methyl addition to thioformaldehyde and found that, while the C-adduct is significantly more stable than the S-adduct (by 41.3 kJ mol^{-1} at 0 K), the reaction barrier for addition to the sulfur is slightly lower (by 5.2 kJ mol^{-1} at 0 K). However, this difference is well within the uncertainty in G2 theory and, in any case, both calculated reaction barriers are relatively low (15.1 kJ mol^{-1} and 20.3 kJ mol^{-1} for the formation of S- and C-adducts, respectively) and so it is difficult to exclude the more stable C-adduct on the basis of these results. Further work is thus required in order to explain why it is the less stable S-adduct that is observed in experimental situations.

In the present study, high-level ab initio molecular orbital calculations of the barriers and reaction enthalpies for methyl radical addition to both the carbon and sulfur centers of CH_2═S, CH_3CH═S, and $(CH_3)_2C$═S have been performed. The barriers for the methyl-transfer reaction that interconverts the S- and C-adducts in each of these systems have also been calculated. The aims of this work are 2-fold. First, it is hoped to establish whether radical addition to C═S double bonds yields the C- or S-adducts, by (a) extending the earlier calculations of Chiu et al.[5] to higher levels of theory, (b) including in the study the radical rearrangement reaction as an alternative means of obtaining the more stable adduct, and (c) including the reactions of the substituted systems (for which any kinetic preference for the S-adduct could be more pronounced). Second, by calculating the barriers and enthalpies for the above reactions at a wide range of moderate to very high levels of theory, it is hoped to establish which levels of theory offer a reasonable compromise between accuracy and computational expense for our subsequent calculations on more complex thiocarbonyl addition reactions.

2. Theoretical Procedures

Standard ab initio molecular orbital theory[7] and density functional theory[8] calculations were carried out using the GAUSSIAN 98,[9] MOLPRO 2000.6,[10] and ACESII 3.0[11] programs. Unless noted otherwise, calculations on radicals were performed with an unrestricted wave function. In cases where a restricted-open-shell wave function has been used, it is designated with an "R" prefix. The frozen-core approximation was used in all calculations except where full calculations (denoted "fu") were required as part of a standard composite method (such as G3[12] or W1[13]). Because the present study is in part an assessment of theoretical procedures, a number of different levels of theory were used for the geometry optimiza-

* Authors to whom correspondence should be addressed. E-mail: radom@rsc.anu.edu.au; mcoote@rsc.anu.edu.au.

10.1021/jp0267656 CCC: $22.00
Published on Web 11/20/2002

tions, zero-point vibrational energy (ZPVE) calculations, and electronic energy calculations. The specific calculations performed are listed and discussed in the Results section with technical details (relating to the various composite procedures used) outlined in the present section.

As part of the assessment, we investigated the performance of the IRCmax method.[14] In this procedure, high-level single-point energy calculations are performed not merely at the transition structure (as in a traditional calculation), but also along the intrinsic reaction coordinate (IRC), with the IRCmax transition structure being then identified as the maximum of these single-point energies. This effectively optimizes the reaction coordinate—which is often the most sensitive part of a transition structure optimization— at the higher level of theory, without the cost of a full optimization at that level of theory. This approach has previously been found to provide excellent approximations to geometries that have been fully optimized at the high level of theory.[14] In performing the IRCmax procedure, IRCs were calculated using the standard GAUSSIAN[9] keyword with a step size of 0.01 bohr·amu$^{0.5}$. In addition, the "very-tight" convergence criteria for both the optimization convergence and SCF convergence were used, as these have been shown to be important in obtaining an accurate description of the reaction path.[15] For cases where there was no barrier (and hence no transition structure) at the low level of theory, a variant of IRCmax called "Scanmax" was used instead. In this procedure, an approximate IRC was obtained by performing a relaxed scan (typically in steps of 0.01 Å) along the forming bond length in the addition reaction—this providing a good approximation to the reaction coordinate in these particular reactions. The accuracy of this approximation was confirmed by calculating both the IRCmax and Scanmax barriers at the CCSD(T)/6-311+G(d,p)//HF/6-31G(d) level of theory for methyl radical addition to both the carbon and sulfur centers of CH_2═S. For both reactions, the IRCmax and Scanmax barriers agree to within 0.1 kJ mol^{-1}, and the forming-bond lengths in the IRCmax and Scanmax transition structures agree to the nearest 0.01 Å.

A number of high-level composite methods were used to calculate improved energies. These include the following: methods from the G3 family such as G3,[12] G3(MP2),[16] G3//B3-LYP,[17] G3(MP2)//B3-LYP,[17] G3X,[18] and G3X(MP2);[18] "RAD" variants[19] of the G3 methods including G3-RAD, G3-(MP2)-RAD, G3X-RAD, and G3X(MP2)-RAD; methods from the CBS family such as CBS-QB3[20] and CBS-RAD;[21] and the W1 theory of Martin et al.[13] using the recently recommended two-point extrapolation procedure.[22] For a detailed description of these procedures, the reader is referred either to the original references or to a recent summary in which the RAD and non-RAD variants are compared.[19]

The majority of these standard methods employ B3-LYP geometry optimizations that, as will be seen below, do not provide very good descriptions of the transition structures for the addition reactions of the present work. To address this problem, two different strategies were employed. In the first strategy, the standard composite methods, using their prescribed geometries and zero-point vibrational energies (ZPVEs, scaled using their prescribed scale factors), were used in conjunction with the IRCmax procedure (as described above). In applying the IRCmax procedure, the IRCmax transition structure was located as the maximum in the non-ZPVE-corrected energies and the ZPVE correction was computed at the improved transition structure and added to the final total energy. In the second strategy, the geometries and accompanying ZPVEs in the standard composite methods were replaced by more accurate calculations of these quantities. For the reactions of methyl radical with CH_2═S, CCSD(T)/6-311+G(d,p) geometry optimizations and QCISD/6-31G(d) ZPVEs (scaled by a factor of 0.9776[23]) were employed, while for the larger systems QCISD/6-31G(d) geometries and ZPVEs were used instead. Less computationally demanding variants of these composite methods, employing HF/6-31G(d) geometries and ZPVEs (scaled by a factor of 0.9135[23]) were also explored. In employing these modified composite methods, the prescribed recipe was followed in all respects other than the geometry optimizations and scaled ZPVE calculations.

In addition to the various composite methods, a number of (low-level) single-point energies were also calculated in an attempt to identify an inexpensive method that could later be applied to larger systems. These single points were typically performed with either HF/6-31G(d) geometries and ZPVEs (scaled by a factor of 0.9135[23]), B3-LYP/6-31G(d) geometries and ZPVEs (scaled by a factor of 0.9806[23]), or MPW1K/6-31+G(d,p) geometries and ZPVEs (scaled by a factor of 0.9515[24]). The calculations with the MPW1K functional were performed in GAUSSIAN using the procedure published by Lynch et al.[25]

To assist in the interpretation of the results, heats of formation for a selection of the stable molecules were calculated with the modified high-level composite methods. These were obtained from the calculated total atomization energies of the stable species and reliable experimental values for the heats of formation of the constituent atoms at 0 K[26] using the procedure published by Nicolaides et al.[27] Whereas the higher-level correction term (HLC) of the G3-type methods cancels from the calculated addition and methyl-transfer barriers and enthalpies, this term does not cancel for the total atomization energies. It is therefore important to select appropriate HLCs for the modified methods. Since the only modifications entail the use of more reliable geometries and ZPVEs, the corresponding standard HLCs are used for the G3X,[18] G3X(MP2),[18] and various "RAD" variants[19] of G3. However, because in the modified methods the QCISD/6-31G(d) frequencies are scaled by a factor designed to reproduce accurate ZPVEs rather than pure vibrational frequencies,[23] the HLC selected for the modified G3 method is the G3//B3-LYP HLC that had been optimized for the scale factor of 0.98.[17] Since there is no published HLC for the G3(MP2)[16] or G3(MP2)//B3-LYP[17] methods appropriate for use in conjunction with scale factors designed to produce ZPVEs (rather than pure vibrational frequencies), this method was omitted from the heats of formation calculations (but was included in the calculations of barriers and enthalpies where the HLC completely cancels).

3. Results and Discussion

A. Geometry Assessment. In the present study, methyl radical addition to a series of prototypical thiocarbonyl compounds (CH_2═S, CH_3CH═S, and $(CH_3)_2C$═S) was examined. The reactants, products, and transition structures for addition at C and S were investigated. Because one of the objectives of this work is to establish whether the S-adduct or C-adduct should be expected as the main product, the methyl-transfer reaction that interconverts these two species was also studied. On the basis of preliminary screening of the possible conformations at the UHF/6-31G(d) level, minimum energy structures for the thiocarbonyl compounds (**1**−**3**, Figure 1), S-centered radical products (**4**−**6**, Figure 2), C-centered radical products (**7**−**10**, Figure 3), C-addition transition structures (**11**−**13**, Figure 4),

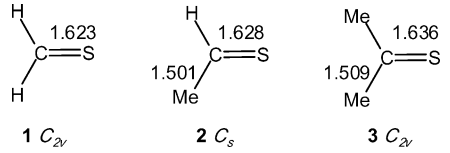

Figure 1. Optimized QCISD/6-31G(d) structures for the thiocarbonyl compounds.

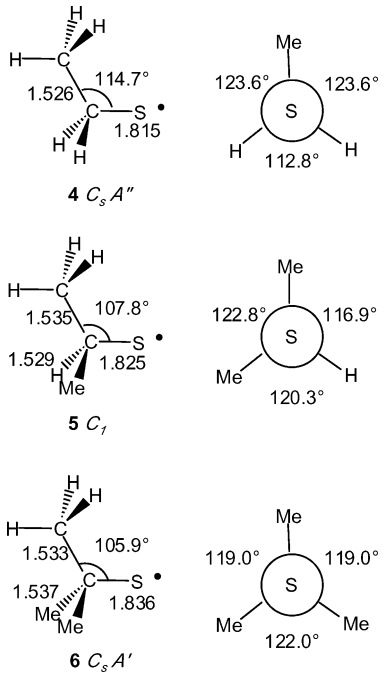

Figure 2. Optimized QCISD/6-31G(d) structures for S-centered radicals (C-adducts).

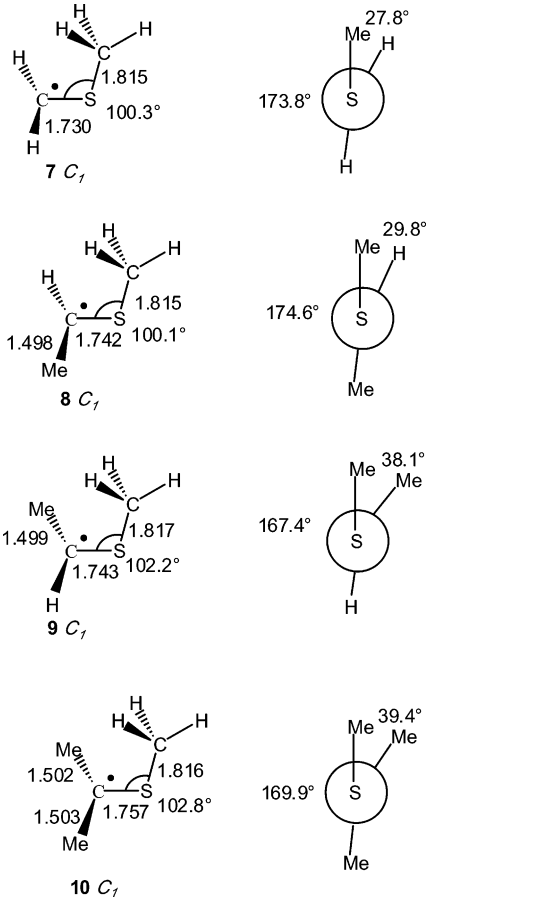

Figure 3. Optimized QCISD/6-31G(d) structures for C-centered radicals (S-adducts).

S-addition transition structures (**14**−**16**, Figure 5), and methyl-transfer transition structures (**17**−**19**, Figure 6) were identified. The more interesting bond lengths (in Å) and bond angles (in degrees) in these structures, based on QCISD/6-31G(d) optimizations, are included in Figures 1−6, while the full QCISD/6-31G(d) geometries are given in the form of GAUSSIAN archive entries in the Supporting Information.

In the case of the $\cdot CH(CH_3)SCH_3$ radical, two minimum energy structures are found, corresponding to anti- and syn-addition (these structures are, respectively, labeled **8** and **9** in Figure 3), with the anti-addition structure **8** being the global minimum. However, owing to the earliness of the addition transition structure, there is only one transition structure for the addition reaction, with the anti and syn C-centered radicals being formed at a later stage in the reaction. The transition structures for the rotation about the $\cdot C-S$ bond which interconverts the anti- and syn-forms of the C-centered radicals are shown in Figure 7 (including those for the $\cdot CH_2SCH_3$ and $\cdot C(CH_3)_2SCH_3$ radicals where the anti- and syn-forms are equivalent).

Having identified the minimum energy conformations for each species, the geometries were re-optimized at a number of additional levels of theory. Single-point energy calculations at the CCSD(T)/6-311+G(d,p) level of theory were then performed on all of the geometries to assess the effect of the geometry optimization level on the reaction barriers and enthalpies. The resulting methyl-radical-addition and -transfer barriers and enthalpies are shown in Tables 1−3 for the $CH_2{=}S$, $CH_3CH{=}S$, and $(CH_3)_2C{=}S$ systems, respectively.

It is clear from Tables 1−3 that the geometry level does not have a major impact on the accuracy of the reaction enthalpies but does affect the reaction barriers. For the addition reactions,

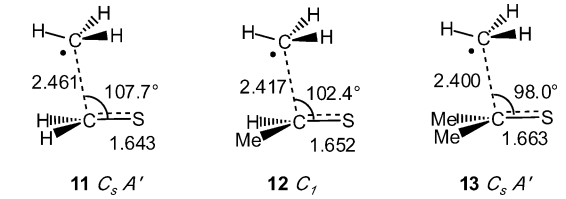

Figure 4. Optimized QCISD/6-31G(d) transition structures for methyl radical addition to C in thiocarbonyl compounds.

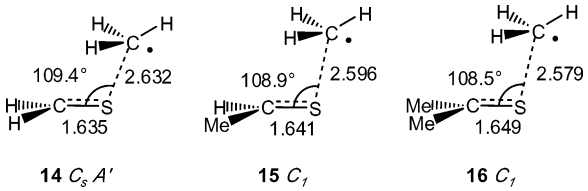

Figure 5. Optimized QCISD/6-31G(d) transition structures for methyl radical addition to S in thiocarbonyl compounds.

the density functional methods perform particularly poorly for the geometry optimizations, leading to underestimates of the reaction barriers by more than 10 kJ mol^{-1} when CCSD(T) single-point energy calculations on these geometries are compared with the full CCSD(T) optimizations. Indeed, in the $CH_2{=}S + \cdot CH_3$ system, there is no barrier at all for addition at S at any of the B3-LYP levels considered, though a transition structure clearly exists at all other levels of theory tested. The geometries obtained using the density functional method MPW1K lead to slightly better estimates of the reaction barrier

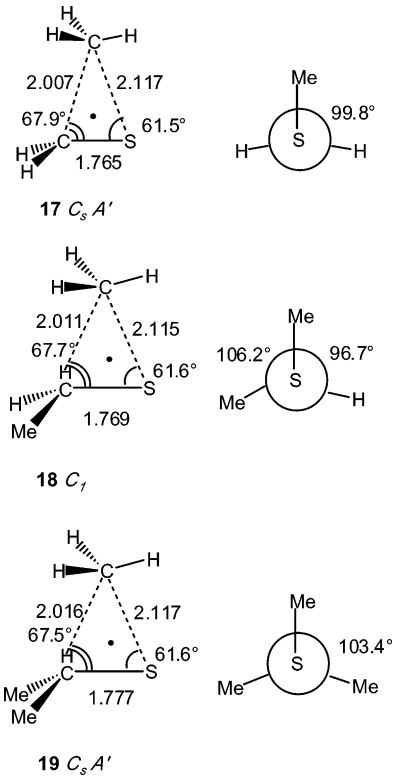

Figure 6. Optimized QCISD/6-31G(d) transition structures for interconversion of the S-centered and C-centered radicals (i.e., methyl transfer).

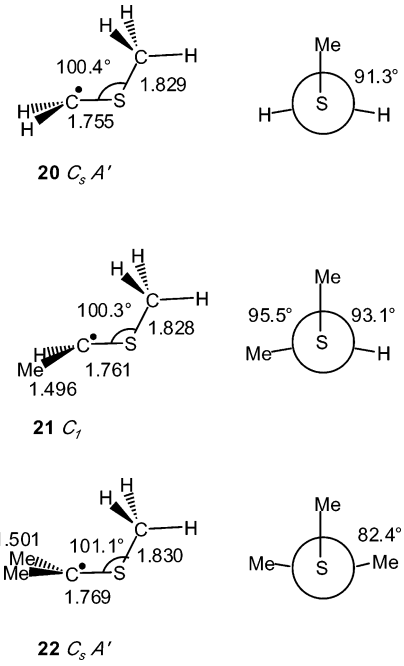

Figure 7. Optimized QCISD/6-31G(d) transition structures for internal rotation about the ·C−S bond in the C-centered radicals.

when compared with those of small-basis B3-LYP optimizations, but the method does not perform as well as the lower-cost HF methods.

The forming bond lengths in both the S-addition and C-addition transition structures are listed as a function of geometry optimization level in Table 4. It is clear that both the B3-LYP and MPW1K methods tend to overestimate the forming bond length in the addition reactions. Indeed, this problem has been observed previously for B3-LYP geometries in the addition

TABLE 1: Effect of Geometry on Methyl-Radical-Addition and Methyl-Transfer Barriers and Enthalpies (CCSD(T)/6-311+G(d,p), kJ mol^{-1}) for the ·CH_3 + CH_2═S System[a]

	add to C		add to S		S· → C·	
geometry	ΔH	$\Delta H^{\ddagger}$	ΔH	$\Delta H^{\ddagger}$	ΔH	$\Delta H^{\ddagger}$
//HF/6-31G(d)	−183.6	9.7	−123.8	9.0	59.8	284.4
//HF/6-311+G(d,p)	−183.6	8.3	−124.0	8.5	59.6	283.1
//MP2/6-31G(d)	−182.1	11.8	−122.8	10.5	59.3	269.5
//MP2/6-311+G(d,p)	−182.2	12.2	−122.7	10.8	59.4	270.1
//MPW1K/6-31+G(d,p)	−182.4	5.7	−123.0	3.0	59.4	266.5
//MPW1K/6-311+G(3df,2p)	−182.9	6.4	−122.4		60.5	266.7
//B3-LYP/6-31G(d)	−181.9	0.3	−122.4	*b*	59.5	266.1
//B3-LYP/6-31G(2df,p)	−182.2	4.3	−122.8	*b*	59.4	265.8
//B3-LYP/6-311+G(d,p)	−182.0	6.9	−122.4	*b*	59.7	266.2
//B3-LYP/6-311+G(3df,2p)	−182.4	7.0	−122.2	*b*	60.2	266.0
//QCISD/6-31G(d)	−182.0	10.4	−122.7	8.9	59.4	266.4
//QCISD/6-311+G(d,p)	−182.1	10.3	−122.8	8.8	59.3	266.3
//CCSD(T)/6-31G(d)	−182.0	10.4	−122.7	9.0	59.4	266.4
//CCSD(T)/6-311+G(d,p)	−182.1	10.4	−122.8	8.9	59.3	266.3
IRCmax//HF/6-31G(d)		10.2		9.0		289.3
IRCmax//B3-LYP/6-31G(d)		10.8		9.1		266.3

[a] The barriers and enthalpies do not include zero-point vibrational energy corrections. [b] Addition to S occurs without a barrier at this level of theory.

TABLE 2: Effect of Geometry on Methyl-Radical-Addition and Methyl-Transfer Barriers and Enthalpies (CCSD(T)/6-311+G(d,p), kJ mol^{-1}) for the ·CH_3 + CH_3CH═S System[a]

	add to C		add to S[b]		S· → C·	
geometry	ΔH	$\Delta H^{\ddagger}$	ΔH	$\Delta H^{\ddagger}$	ΔH	$\Delta H^{\ddagger}$
//HF/6-31G(d)	−168.5	14.2	−107.7	11.0	60.8	269.4
//HF/6-311+G(d,p)	−168.6	12.5	−107.9	10.0	60.7	268.6
//MP2/6-31G(d)	−167.8	17.1	−107.2	12.9	60.6	258.1
//MP2/6-311+G(d,p)	−167.8	17.4	−107.1	13.0	60.7	258.8
//MPW1K/6-31+G(d,p)	−168.2	13.6	−107.4	7.3	60.8	255.2
//MPW1K/6-311+G(3df,2p)	−168.8	13.8	−106.9	6.8	61.9	255.6
//B3-LYP/6-31G(d)	−167.6	13.7	−106.7	5.5	60.9	255.0
//B3-LYP/6-31G(2df,p)	−168.0	14.0	−106.9	5.4	61.1	254.8
//B3-LYP/6-311+G(d,p)	−167.7	14.6	−106.8	8.2	60.9	255.1
//B3-LYP/6-311+G(3df,2p)	−168.2	14.5	−106.7	7.1	61.6	255.1
//QCISD/6-31G(d)	−167.7	15.6	−107.1	11.2	60.6	254.9
//QCISD/6-311+G(d,p)	−167.7	15.5	−107.2	11.0	60.5	254.8
//CCSD(T)/6-31G(d)	−167.7	15.6	−107.1	11.2	60.6	254.9
IRCmax//HF/6-31G(d)		15.7		11.0		
IRCmax//B3-LYP/6-31G(d)		16.4		12.9		

[a] The barriers and enthalpies do not include zero-point vibrational energy corrections. [b] Results correspond to production of the anti-conformation (**8**) of the •$CH(CH_3)SCH_3$ radical.

of methyl radicals to C═C bonds,[28] though the effect in that situation is much smaller. It is likely that the problem is exacerbated for the present C═S addition reactions because they have much smaller barriers and earlier (and thus looser) transition structures. This is supported by the observation that, within the present results, the effect diminishes somewhat with methyl substitution and upon going from the S-adduct transition structures to the C-adduct transition structures—changes that raise the reaction barrier and lead to a later transition structure.

The relatively poor performance of the B3-LYP methods for estimating the geometries of transition structures in addition reactions involving C═S double bonds may, at first glance, appear to be a major setback. This is because B3-LYP optimizations are often prescribed as part of high-level composite methods such as W1, CBS-QB3, and G3-RAD. Furthermore, the high-level composite methods that dispense with B3-LYP optimizations, do so in favor of more expensive levels of theory, such as MP2(fu)/6-31G(d) (in the case of G3) or QCISD/6-31G(d) (in the case of CBS−RAD//QCI), and these levels are often too computationally expensive for all but the simplest

TABLE 3: Effect of Geometry on Methyl-Radical-Addition and Methyl-Transfer Barriers and Enthalpies (CCSD(T)/6-311+G(d,p), kJ mol^{-1}) for the $\cdot CH_3 + (CH_3)_2C{=}S$ System[a]

	add to C		add to S		S• → C•	
geometry	ΔH	$\Delta H^{\ddagger}$	ΔH	$\Delta H^{\ddagger}$	ΔH	$\Delta H^{\ddagger}$
//HF/6-31G(d)	−160.1	17.3	−97.6	11.4	62.5	264.1
//HF/6-311+G(d,p)	−160.3	15.5	−97.9	10.1	62.4	263.2
//MP2/6-31G(d)	−159.7	21.3	−98.0	13.6	61.7	248.0
//MP2/6-311+G(d,p)	−159.7	21.6	−98.0	13.6	61.8	249.0
//MPW1K/6-31+G(d,p)	−160.2	18.9	−97.9	9.2	62.3	245.2
//MPW1K/6-311+G(3df,2p)	−160.7	18.8	−97.3		63.5	245.7
//B3-LYP/6-31G(d)	−159.4	19.3	−96.8	7.8	62.7	245.1
//B3-LYP/6-31G(2df,p)	−159.8	19.2	−96.6	7.7	63.3	245.1
//B3-LYP/6-311+G(d,p)	−159.5	19.7	−97.1	9.9	62.5	245.3
//B3-LYP/6-311+G(3df,2p)	−160.1	19.5	−96.8	9.0	63.3	245.4
//QCISD/6-31G(d)	−159.6	19.7	−97.7	11.9	61.9	244.8
//QCISD/6-311+G(d,p)	−159.6	19.7	−98.0		61.6	
IRCmax//HF/6-31G(d)		19.9		11.7		
IRCmax//B3-LYP/6-31G(d)		20.5		13.8		

[a] The barriers and enthalpies do not include zero-point vibrational energy corrections.

systems. Fortunately, however, the IRCmax procedure[14] offers a cost-effective means of improving the transition structure geometries in the addition reactions. This was confirmed by calculating IRCmax reaction barriers with single-point energies at CCSD(T)/6-311+G(d,p) (the same high level of theory that was used to test the other geometry optimization levels) using both the HF/6-31G(d) and B3-LYP/6-31G(d) optimized reaction paths. The resulting barriers are included in Tables 1−3, and the forming bond lengths obtained by the IRCmax procedure are included in Table 4. It is clear from these results that the IRCmax procedure leads to greatly improved estimates for the forming bond lengths in the B3-LYP transition structures and more modest improvements in the HF transition structure geometries (which are reasonably accurate to start with). As a result, the IRCmax barriers for both surfaces are very close to the fully optimized barriers at the high level of theory and, in the case of the B3-LYP optimizations, this represents an improvement of more than 10 kJ mol^{-1} in some cases. Hence, the B3-LYP methods can yield good estimates of the geometries, provided that the transition structures are optimized with an IRCmax procedure.

For the methyl-transfer barriers, it is the HF geometries—and not the DFT methods—that provide poor approximations to the higher-level geometries, with errors of up to 18 kJ mol^{-1}. The forming and breaking bond lengths for the methyl-transfer transition structures are shown in Table 5 for selected levels of theory. From these results it is clear that, while the B3-LYP/6-31G(d) level offers excellent approximations to the high-level UCCSD(T)/6-31G(d) geometries, the UHF/6-31G(d) level overestimates both the forming and breaking bond-lengths by up to 0.4 Å. This is not a major problem for the present work as none of the standard composite methods that are used to estimate the energies employ UHF procedures for the optimization of the geometry. Nonetheless, given the success of the IRCmax

TABLE 4: Effect of Level of Theory on the Forming C···C Bond or C···S Bond in the Methyl-Radical-Addition Transition Structures[a]

	forming C···C bond			forming C···S bond		
geometry	**11**	**12**	**13**	**14**	**15**	**16**
//HF/6-31G(d)	2.440	2.369	2.337	2.678	2.593	2.549
//HF/6-311+G(d,p)	2.398	2.508	2.316	2.618	2.550	2.511
//MP2/6-31G(d)	2.500	2.420	2.388	2.676	2.591	2.549
//MP2/6-311+G(d,p)	2.494	2.419	2.392	2.664	2.585	2.544
//MPW1K/6-31+G(d,p)	2.715	2.527	2.470	3.036	2.830	2.756
//MPW1K/6-311+G(3df,2p)	2.656	2.497	2.447		2.839	2.764
//B3-LYP/6-31G(d)	2.919	2.571	2.510	*b*	2.967	2.863
//B3-LYP/6-31G(2df,p)	2.810	2.542	2.489	*b*	2.955	2.851
//B3-LYP/6-311+G(d,p)	2.697	2.529	2.483	*b*	2.822	2.762
//B3-LYP/6-311+G(3df,2p)	2.671	2.513	2.468	*b*	2.856	2.785
//QCISD/6-31G(d)	2.461	2.417	2.400	2.632	2.596	2.579
//QCISD/6-311+G(d,p)	2.459	2.418	2.404	2.632	2.597	
//CCSD(T)/6-31G(d)	2.478	2.432		2.640	2.606	
//CCSD(T)/6-311+G(d,p)	2.480			2.650		
IRCmax at CCSD(T)/6-311+G(d,p):						
//HF/6-31G(d)	2.49	2.45	2.43	2.67	2.62	2.60
//B3-LYP/6-31G(d)	2.48	2.43	2.43	2.63	2.57	2.55

[a] Bond lengths are in Å and structure numbers refer to the transition structures shown in Figures 4 and 5. [b] Addition to S occurs without a barrier at this level of theory.

TABLE 5: Effect of Level of Theory on the Forming (C···S) and Breaking (C···C) Bonds in the Methyl-Transfer Transition Structures[a]

	17		**18**		**19**	
geometry	C···S	C···C	C···S	C···C	C···S	C···C
//HF/6-31G(d)	2.385	2.246	2.384	2.440	2.387	2.245
//MP2/6-31G(d)	2.028	1.912	2.024	1.915	2.025	1.919
//MPW1K/6-31+G(d,p)	2.067	1.960	2.067	1.967	2.070	1.975
//MPW1K/6-311+G(3df,2p)	2.055	1.955	2.055	1.961	2.059	1.968
//B3-LYP/6-31G(d)	2.115	2.016	2.121	2.027	2.129	2.039
//QCISD/6-31G(d)	2.117	2.007	2.115	2.011	2.117	2.016
//CCSD(T)/6-31G(d)	2.114	2.008	2.114	2.008		
IRCmax at CCSD(T)/6-311+G(d,p):						
//HF/6-31G(d)	2.373	2.271				
//B3-LYP/6-31G(d)	2.119	2.009				

[a] Bond lengths are in Å and structure numbers refer to the transition structures shown in Figure 6.

TABLE 6: Effect of Level of Theory on the Contribution of Scaled Zero-Point Vibrational Energies (kJ mol^{-1}) to the Methyl-Radical-Addition and Methyl-Transfer Barriers and Enthalpies for the $\cdot CH_3 + CH_2{=}S$ System[a]

		add to C		add to S		S• → C•	
level of theory	scale factor	ΔH	$\Delta H^{\ddagger}$	ΔH	$\Delta H^{\ddagger}$	ΔH	$\Delta H^{\ddagger}$
HF/6-31G(d)	0.9135	28.7	10.3	19.9	7.2	−8.8	−15.5
HF/6-311+G(d,p)	0.9248	28.6	10.3	19.3	7.2	−9.3	−6.7
MP2/6-31G(d)	0.9670	27.9	11.0	20.1	8.8	−7.7	−0.3
MP2/6-311+G(d,p)	0.9748	26.4	10.0	18.9	7.9	−7.5	−0.4
MPW1K/6-31+G(d,p)	0.9515	26.5	6.7	17.7	4.1	−8.7	−0.6
MPW1K/6-311+G(3df,2p)	0.9515	26.0	6.8	17.4		−8.6	−0.7
B3-LYP/6-31G(d)	0.9806	26.8	5.7	18.9	*b*	−7.9	−1.7
B3-LYP/6-31G(2df,p)	0.9854	26.0	6.4	18.3	*b*	−7.7	−1.8
B3-LYP/6-311+G(d,p)	0.9806	26.1	7.4	17.7	*b*	−8.4	−1.4
B3-LYP/6-311+G(3df,2p)	0.9806	25.7	7.4	17.2	*b*	−8.6	−1.1
QCISD/6-31G(d)	0.9776	28.7	10.5	20.1	8.2	−8.6	−1.7
QCISD/6-311+G(d,p)	0.9776	27.5	9.6	19.1	7.1	−8.4	−1.6
CCSD(T)/6-31G(d)	0.9776	28.2	10.4	19.9	7.8	−8.2	−1.9
IRCmax at CCSD(T)/6-311+G(d,p): //B3-LYP/6-31G(d)	0.9806		10.7		7.2		

[a] Computed using geometries optimized at the same level of theory and scaled using previously published[18,23] scale factors. For the 6-311+G(d,p) and 6-311+G(3df,2p) basis sets, scale factors are not available and the corresponding 6-311G(d,p) scale factors (in the case of the HF and MP2 methods) or 6-31G(d) scale factors (in the case of the QCISD and B3-LYP methods) are used instead. No appropriate scale factors for CCSD(T) frequencies are available so the QCISD/6-31G(d) scale factor is used instead. [b] Addition to S occurs without a barrier at this level of theory.

procedure for improving the B3-LYP transition structures in the addition reactions, it is of interest to explore whether this approach could also improve the HF methyl-transfer transition structures.

IRCmax methyl-transfer barriers were calculated with the B3-LYP/6-31G(d) and HF/6-31G(d) surfaces for the $CH_3CH_2S\cdot \rightarrow \cdot CH_2SCH_3$ reaction. The resulting barriers are included in Table 1, and the lengths of the forming and breaking bonds corresponding to the IRCmax transition structures for each surface are included in Table 5. From these results it appears that the IRCmax procedure fails to improve the HF geometries for these reactions, with the forming and breaking bonds remaining too long and the error in the reaction barrier actually increasing by 4.9 kJ mol^{-1}. For the B3-LYP/6-31G(d) surface, the IRCmax barrier reproduces the fully optimized barrier to the nearest 0.1 kJ mol^{-1}. However, since the original B3-LYP/6-31G(d) optimization itself differs from the high-level result by only 0.2 kJ mol^{-1}, the IRCmax procedure is not critically tested in this case.

The IRCmax procedure thus improves the B3-LYP methyl-radical-addition transition structures, but not the HF methyl-transfer transition structures. This can be explained as follows. In both cases, the low-level methods obtain incorrect estimates for the stretched bonds in the transition structure, which the IRCmax procedure attempts to re-optimize at the high level of theory. This is successful for the methyl-radical-addition transition structures because they contain just one stretched bond (the forming C···C bond), the length of which provides a good first approximation to the reaction coordinate. As a result, all possible stretched bond lengths are accessible along the reaction path and hence the IRCmax procedure is able to optimize the stretched bond at the high level of theory. In contrast, the methyl-transfer transition structures contain two stretched bonds (the breaking C···C and the forming C···S bonds) and, while the lengths of both of these bonds vary as a function of the reaction coordinate, their values are coupled with one another and with a range of other parameters (such as the bond angles involving the carbon of the transferred methyl group and the carbon and sulfur centers between which it is transferred). As a result, only certain combinations of the two stretched bond lengths are accessible along the reaction coordinate, and it is therefore not possible to optimize these fully at the high level of theory.

In summary, the barriers and enthalpies for the methyl-radical-addition and -transfer reactions considered in the present work are, in general, relatively insensitive to the level of theory selected for the geometry optimization. However, there are two important exceptions to this. First, in the addition reactions, the DFT methods (B3-LYP and MPW1K) overestimate the forming bond length and significantly underestimate the barrier. This problem can be overcome by using an IRCmax (or Scanmax) procedure. Second, in the transfer reactions, the HF methods overestimate both the forming and breaking bond lengths in the reaction barrier. For these reactions, B3-LYP (or higher) methods should be used for the geometry optimizations.

B. Zero-Point Vibrational Energy Assessment. The zero-point vibrational energy contribution (scaled using standard scale factors[23]) to the barriers and enthalpies of the $\cdot CH_3 + CH_2{=}S$ system are shown in Table 6. From these results, it can be seen that the effect of level of theory on the zero-point vibrational energies is relatively small. Furthermore, the main differences that do occur mirror those in the geometry optimizations, with the DFT methods (B3-LYP and MPW1K) performing poorly for the methyl-radical-addition barriers and the HF levels performing poorly for the methyl-transfer barriers. Because the majority of standard composite methods prescribe B3-LYP/6-31G(d) zero-point vibrational energies, and because the higher-level alternatives would not be feasible for larger systems, it is helpful to identify a low-cost solution to this problem. One possible solution is to use the lower-level HF/6-31G(d) frequencies (on HF/6-31G(d) geometries) for the addition reactions as these appear to provide adequate approximations to the higher-level methods (see Table 6). Another possibility is to calculate the B3-LYP zero-point vibrational energies at the IRCmax transition structure in the addition reactions. When this is done, the zero-point vibrational energy contribution to the reaction barrier is in good agreement with the other levels of theory (see Table 6). In conclusion, provided appropriate scale factors are used, the zero-point vibrational energy is relatively independent of the level of theory. However, it is important that HF methods are not used for the methyl-transfer barriers and that DFT methods such as B3-LYP are applied at the IRCmax transition structures in the methyl-radical-addition reactions.

C. Energy Assessment. Barriers and enthalpies, at various levels of theory, for methyl radical addition to both the S- and C-centers of $CH_2{=}S$, $CH_3CH{=}S$ and $(CH_3)_2C{=}S$ are shown

TABLE 7: Effect of Level of Theory on the Barriers and Enthalpies (0 K, kJ mol^{-1}) for Methyl-Radical-Addition and Methyl-Transfer Reactions in the $\cdot CH_3 + CH_2{=}S$ System[a]

	add to C		add to S		S• → C•	
level of theory	ΔH	$\Delta H^{\ddagger}$	ΔH	$\Delta H^{\ddagger}$	ΔH	$\Delta H^{\ddagger}$
Low-Level Methods						
B3-LYP/6-31G(d)//HF	−167.9	−0.4	−114.7	−1.5	53.1	259.3
B3-LYP/6-311+G(3df,2p)//HF	−148.3	9.1	−114.0	5.1	34.3	249.1
RB3-LYP/6-311+G(3df,2p)//HF	−148.1	14.3	−113.5	10.6	34.6	
RMP2/6-311+G(3df,2p)//HF	−163.8	22.4	−118.2	13.9	45.6	260.7
B3-LYP/6-31G(d)//B3	−168.8	2.0	−115.1	*b*	53.8	248.1
B3-LYP/6-311+G(3df,2p)//B3	−149.8	6.2	−115.8	*b*	34.0	237.3
RB3-LYP/6-311+G(3df,2p)//B3	−150.2	6.5	−114.9	*b*	35.2	240.9
RMP2/6-311+G(3df,2p)//B3	−165.3	3.5	−120.2	*b*	45.1	244.6
MPW1K/6-31+G(d,p)//MPW1	−188.3	6.4	−139.6	3.9	48.7	260.7
MPW1K/6-311+G(3df,2p)//MPW2	−181.5	7.7	−145.7		35.8	250.8
Cheap Composite Methods						
CBS-RAD//HF	−156.2	7.7	−117.8	3.1	38.3	255.1
G3(MP2)-RAD//HF	−151.7	15.3	−110.8	9.8	40.9	247.5
G3X//HF	−152.0	18.6	−112.1	13.6	40.0	261.2
Standard Composite Methods						
CBS-QB3	−157.5	4.9	−120.5	*b*	37.1	236.4
CBS-RAD (B3,B3)	−157.2	3.6	−119.0	*b*	38.2	236.9
CBS-RAD (QCI,QCI)	−155.7	7.4	−118.1	1.5	37.6	236.2
G3(MP2)-RAD	−152.4	4.8	−111.7	*b*	40.7	238.3
G3X(MP2)-RAD	−153.3	6.9	−114.2	*b*	39.1	237.8
G3-RAD	−157.5	4.5	−114.4	*b*	43.1	243.5
G3X-RAD	−158.5	6.6	−116.5	*b*	41.9	242.9
G3(MP2)//B3-LYP	−152.3	5.5	−112.6	*b*	39.7	242.1
G3MP2	−150.9	20.3	−112.6	13.6	38.3	239.2
G3X(MP2)	−152.7	8.7	−114.6	*b*	38.0	241.3
G3//B3-LYP	−153.9	5.2	−113.5	*b*	40.4	243.3
G3	−152.5	17.5	−113.6	10.8	38.9	240.4
G3X	−154.3	8.1	−115.1	*b*	39.2	242.7
IRCmax Composite Methods						
IRCmax CBS−RAD (B3,B3)		7.9		1.2		
IRCmax G3(MP2)-RAD		15.9		8.3		
High-Level Composite Methods						
CBS-QB3//CC	−155.9	7.2	−119.0	1.4	36.9	235.9
CBS-RAD//CC	−155.8	7.5	−118.9	1.7	36.9	235.9
G3(MP2)-RAD//CC	−150.9	15.3	−111.5	9.1	39.4	236.8
G3X(MP2)-RAD//CC	−150.6	15.3	−112.2	9.0	38.3	236.3
G3-RAD//CC	−156.2	14.6	−114.4	9.2	41.7	242.1
G3X-RAD//CC	−156.0	14.6	−114.9	9.1	41.2	241.5
G3(MP2)//CC	−150.2	19.8	−111.9	14.0	38.3	240.8
G3X(MP2)//CC	−150.0	19.8	−112.7	13.8	37.2	240.3
G3//CC	−151.9	17.1	−113.1	11.3	38.9	242.1
G3X//CC	−151.9	17.1	−113.4	11.2	38.5	241.8
W1//CC	−158.5	13.7	−123.4	8.2	35.1	239.7

[a] In this and succeeding tables: //HF means HF/6-31G(d) geometries and ZPVEs; //B3 means B3-LYP/6-31G(d) geometries and ZPVEs; //MPW1 means MPW1K/6-31+G(d,p) geometries and ZPVEs; //MPW2 means MPW1K/6-311+G(3df,2p) geometries and MPW1K/6-31+G(d,p) ZPVEs; //QCI means QCISD/6-31G(d) geometries and ZPVEs; //CC means CCSD(T)/6-311+G(d,p) geometries and QCISD/6-31G(d) ZPVEs. The standard composite methods use their prescribed geometries and ZPVEs. [b] Addition to S occurs without a barrier at this level of theory.

in Tables 7, 8, and 9, respectively. Corresponding barriers and enthalpies for the methyl-transfer reaction that interconverts the S-centered and C-centered radicals are also included in Tables 7−9, for the respective systems. As noted above, the majority of standard composite methods prescribe B3-LYP methods for optimizing the geometries and calculating the zero-point vibrational energies (ZPVEs)—methods that are not suitable for describing the transition structures in the addition reactions of the present systems. Given this problem, various modifications to the standard composite methods were examined with a view to establishing which methods provide accurate barriers and enthalpies, and which (if any) computationally inexpensive methods could provide reasonable approximations to the high-level results. With this objective, the wide range of methods used to calculate the enthalpies and barriers in Tables 7−9 can be loosely grouped into the following categories: (1) the *high-level composite methods* (in which the standard composite methods are applied using the best available geometries and ZPVEs); (2) *IRCmax composite methods* (in which the IRCmax technique is applied to the standard composite methods using their prescribed geometries and ZPVEs); (3) *standard composite methods* (applied using their prescribed methods, typically B3-LYP, for geometries and ZPVEs); (4) *cheap composite methods* (in which the standard composite methods are applied to HF/6-31G(d) geometries and ZPVEs since these were shown to outperform the B3-LYP geometries for the addition transition structures); (5) *low-level methods* (consisting of various ZPVE-corrected low-level single-point energies). In what follows, each of these groups of methods is discussed.

High-Level Composite Methods. Our initial goal was to establish which are the best estimates of the barriers and enthalpies for the various reactions and which composite methods are able to reproduce them. To this end, a wide variety of composite methods were applied using the best available

TABLE 8: Effect of Level of Theory on the Barriers and Enthalpies (0 K, kJ mol^{-1}) for Methyl-Radical-Addition and Methyl-Transfer Reactions in the $\cdot CH_3 + CH_3CH{=}S$ System[a]

	add to C		add to S		S• → C•	
level of theory	ΔH	$\Delta H^{\ddagger}$	ΔH	$\Delta H^{\ddagger}$	ΔH	$\Delta H^{\ddagger}$
Low-Level Methods						
B3-LYP/6-31G(d)//HF	−138.2	11.9	−95.9	1.4	42.3	236.7
B3-LYP/6-311+G(3df,2p)//HF	−118.6	22.0	−92.8	7.8	25.9	226.9
RB3-LYP/6-311+G(3df,2p)//HF	−118.5	27.6	−92.4	14.2	26.1	228.0
RMP2/6-311+G(3df,2p)//HF	−145.4	31.2	−99.1	17.3	46.3	242.0
B3-LYP/6-31G(d)//B3	−137.8	15.4	−97.3	3.4	40.5	226.0
B3-LYP/6-311+G(3df,2p)//B3	−119.0	21.8	−95.3	6.2	23.8	215.8
RB3-LYP/6-311+G(3df,2p)//B3	−118.9	23.8	−94.8	7.0	24.0	218.5
RMP2/6-311+G(3df,2p)//B3	−145.9	18.9	−101.5	3.5	44.4	229.0
MPW1K/6-31+G(d,p)//MPW1	−159.1	17.6	−118.8	7.5	40.4	241.3
MPW1K/6-311+G(3df,2p)//MPW2	−152.3	19.4	−124.1	7.1	28.3	232.0
Cheap Composite Methods						
CBS-RAD//HF	−137.7	14.7	−101.6	4.5	36.0	234.7
G3(MP2)-RAD//HF	−134.5	21.7	−93.9	11.6	40.5	232.2
G3X//HF	−134.5	24.8	−94.8	15.1	39.7	239.3
Standard Composite Methods						
CBS-QB3	−139.5	13.7	−104.4	0.5	35.1	221.5
CBS-RAD (B3,B3)	−137.8	12.9	−103.6	−0.2	34.2	220.2
G3(MP2)-RAD	−134.3	18.0	−95.6	4.4	38.7	223.5
G3X	−135.7	20.5	−98.5	5.2	37.3	227.8
High-Level Composite Methods						
CBS-RAD//QCI	−138.1	14.4	−102.8	3.0	35.3	221.4
G3(MP2)-RAD//QCI	−134.5	21.3	−94.7	10.7	39.8	224.0
G3X//QCI	−135.1	23.4	−96.1	12.7	39.0	228.7
approximate W1[b]	−142.0	19.7	−106.5	9.8	35.5	226.9

[a] See footnote *a* from Table 7. [b] The "approximate W1" estimates were obtained by adding the substituent effect, as calculated with the high-level G3(MP2)-RAD//QCI method (Table 10), to the corresponding W1//CC estimates of the barriers and enthalpies for the unsubstituted system from Table 7.

TABLE 9: Effect of Level of Theory on the Barriers and Enthalpies (0 K, kJ mol^{-1}) for Methyl-Radical-Addition and Methyl-Transfer Reactions in the $\cdot CH_3 + (CH_3)_2C{=}S$ System[a]

	add to C		add to S		S• → C•	
level of theory	ΔH	$\Delta H^{\ddagger}$	ΔH	$\Delta H^{\ddagger}$	ΔH	$\Delta H^{\ddagger}$
Low-Level Methods						
B3-LYP/6-31G(d)//HF	−117.6	24.0	−81.9	3.2	35.8	219.1
B3-LYP/6-311+G(3df,2p)//HF	−98.0	35.0	−75.9	9.4	22.1	209.6
RB3-LYP/6-311+G(3df,2p)//HF	−97.8	40.6	−75.6	16.0	22.2	209.9
RMP2/6-311+G(3df,2p)//HF	−134.7	39.2	−83.4	19.0	51.3	228.2
B3-LYP/6-31G(d)//B3	−118.8	27.2	−84.1	6.1	34.7	211.6
B3-LYP/6-311+G(3df,2p)//B3	−99.9	35.0	−79.2	9.0	20.7	202.2
RB3-LYP/6-311+G(3df,2p)//B3	−99.8	37.7	−78.9	10.4	20.9	204.6
RMP2/6-311+G(3df,2p)//B3	−136.9	27.9	−86.7	6.7	50.2	221.1
MPW1K/6-31+G(d,p)//MPW1	−140.5	28.5	−102.8	10.3	37.7	227.6
MPW1K/6-311+G(3df,2p)//MPW2	−132.9	31.2	−106.8	9.8	26.1	218.5
Cheap Composite Methods						
CBS-RAD//HF	−128.4	19.9	−88.1	4.7	40.2	226.4
G3(MP2)-RAD//HF	−124.3	27.7	−80.3	12.5	44.0	221.2
G3X//HF	−124.2	30.8	−80.8	15.7	43.3	227.7
Standard Composite Methods						
CBS-QB3	−129.5	20.8	−91.8	2.5	37.7	211.3
CBS-RAD (B3,B3)	−130.1	19.4	−91.4	1.9	38.7	214.7
G3(MP2)-RAD	−125.8	25.3	−82.8	7.1	43.0	215.4
G3X	−127.1	27.5	−85.1	7.8	42.0	218.9
High-Level Composite Methods						
CBS-RAD//QCI	−129.6	20.0	−90.7	3.6	38.9	214.1
G3(MP2)-RAD//QCI	−125.1	27.4	−82.2	11.6	42.9	214.0
G3X//QCI	−125.5	29.6	−83.2	13.4	42.3	218.5
approximate W1[b]	−132.7	25.8	−94.0	10.7	38.7	216.9

[a] See footnote *a* from Table 7. [b] See footnote *b* from Table 8.

geometries and ZPVEs for each of the systems. Examining the high-level results in Tables 7−9, it can be seen that all of the high-level methods are in reasonable agreement with one another for both the enthalpies and barriers in both the methyl-radical-addition and -transfer reactions, with the maximum differences among the various estimates for a given quantity generally not exceeding 10 kJ mol^{-1} (except in the case of the $\cdot CH_3 + CH_2{=}S$ addition barriers where variations of up to 13 kJ mol^{-1} are observed). Furthermore, on comparing the methyl-substituted and unsubstituted systems, the estimates for the relative barriers

TABLE 10: Effect of Level of Theory on the Relative Barriers and Enthalpies (0 K, kJ mol^{-1}) for Methyl-Radical-Addition and Methyl-Transfer in the $\cdot CH_3$ + CXY=S (X, Y = H or CH_3) Systems[a]

	add to C		add to S		S• → C•	
level of theory	ΔH	$\Delta H^{\ddagger}$	ΔH	$\Delta H^{\ddagger}$	ΔH	$\Delta H^{\ddagger}$
			Effect of One Methyl Substituent[b]			
MPW1K/6-31+G(d,p)//MPW1	29.2	11.2	20.8	3.7	−8.3	−19.4
B3-LYP/6-311+G(3df,2p)//B3	30.7	12.9[c]	20.5	2.7[c]	−10.2	−21.4
RB3-LYP/6-311+G(3df,2p)//B3	31.3	13.3[c]	20.1	3.6[c]	−11.2	−22.4
RMP2/6-311+G(3df,2p)//B3	19.4	8.9[c]	18.7	3.5[c]	−0.8	−15.6
CBS-RAD//QCI [e]	17.7	6.9	16.1	1.3	−1.6	−14.5
G3(MP2)-RAD//QCI [e]	16.4	6.1	16.9	1.6	0.4	−12.8
G3X//QCI[e]	16.8	6.3	17.3	1.5	0.6	−13.1
			Effect of Two Methyl Substituents[d]			
MPW1K/6-31+G(d,p)//MPW1	47.8	22.1	36.8	6.4	−11.0	−33.1
B3-LYP/6-311+G(3df,2p)//B3	49.8	25.9[c]	36.6	4.3[c]	−13.3	−35.1
RB3-LYP/6-311+G(3df,2p)//B3	50.4	26.4[c]	36.0	5.3[c]	−14.3	−36.3
RMP2/6-311+G(3df,2p)//B3	28.4	16.8[c]	33.5	5.1[c]	5.1	−23.4
CBS-RAD//QCI [e]	26.2	12.5	28.1	1.9	1.9	−21.9
G3(MP2)-RAD//QCI [e]	25.8	12.1	29.3	2.5	3.5	−22.8
G3X//QCI [e]	26.3	12.4	30.2	2.3	3.9	−23.3

[a] See footnote *a* from Table 7. [b] Defined as the difference between corresponding barriers or enthalpies in the monomethyl- and unsubstituted systems. [c] Calculated with HF/6-31G(d) geometries and ZPVEs (see text). [d] Defined as the difference between corresponding barriers or enthalpies in the dimethyl- and unsubstituted systems. [e] The unsubstituted system was actually calculated with CCSD(T)/6-311+G(d,p) geometries.

and enthalpies among the different high-level methods, shown in Table 10, differ by less than 2 kJ mol^{-1} and hence for relative barriers and enthalpies, any of the composite methods appear to be acceptable. The various high-level methods are also in close agreement when the energy difference between the barriers for addition to the S- and C-centers of the C=S bond are examined. For these relative barriers, the maximum variation in the $\cdot CH_3 + CH_2$=S system is just 1 kJ mol^{-1}.

To reduce further the uncertainty in the absolute barriers and enthalpies, it is necessary to compare the methods more closely. For the unsubstituted system, it was possible to include calculations with the W1 theory of Martin et al.[13] which, because it extrapolates to an infinite basis set using restricted-open-shell coupled-cluster energies, would reasonably be expected to provide the most accurate barriers and enthalpies among the present methods. When the results with the other high-level composite methods are benchmarked against W1, the following patterns emerge.

For the addition reactions, the barriers for W1 and the "RAD" variants of the G3-type methods are in reasonable agreement with one another, with the non-RAD variants of G3 giving barriers up to 6 kJ mol^{-1} higher than W1 and the CBS-type methods giving barriers that are lower by around 7 kJ mol^{-1}. This suggests that the non-RAD G3-type methods overestimate the barrier while the CBS-type methods underestimate the barrier. This behavior may be associated with variable spin contamination in the addition reactions. While the product and reactant radicals in the addition reactions are not significantly spin contaminated (with $\langle S^2 \rangle$ values of 0.76−0.77 at MP2/6-311+G(3df,2df,2p),[29] compared with the 0.75 required for a pure doublet radical), the transition structures have relatively high $\langle S^2 \rangle$ values (around 1.1 for the methyl-radical-addition transition structures and 0.92 for the methyl-transfer transition structures). Hence, errors arising from spin contamination would not be expected to cancel from the reaction barriers and must be dealt with explicitly. The different groups of methods deal with spin contamination in different ways. W1 and the "RAD" variants of G3 avoid spin contamination by using restricted-open-shell wave functions. In contrast, the non-RAD G3-type methods use unrestricted wave functions, do not include any spin-contamination-correction terms and hence do not account for spin contamination. This could explain why the non-RAD G3-type methods overestimate the reaction barrier. The CBS-type methods also use unrestricted wave functions but include a spin-contamination-correction term which is evaluated from the difference between the ideal and actual $\langle S^2 \rangle$ values, multiplied by an empirically based pre-factor.[30] In the addition barriers of the present work, this term accounts for approximately 9 kJ mol^{-1} of the difference between the CBS-type and other methods. In contrast, the difference between corresponding RAD and non-RAD versions of G3 or G3X is approximately 3 kJ mol^{-1}. If this difference is used as an alternative estimate of the spin-contamination error, it could be suggested that the CBS-type methods are over-estimating the spin-correction term by around 6 kJ mol^{-1}—which is very close to the difference between the W1 and CBS-type methods. This is consistent with the observation that, when the spin contamination is negligible (as in the reaction enthalpies for addition and transfer), the CBS-type and W1 methods are in much better agreement (within 3 kJ mol^{-1}). It is thus possible that, for the present systems, the empirical pre-factor in the spin-contamination-correction term of the CBS-type methods (which had been optimized for the C−H dissociation energies of HCN, C_2H_4, and C_2H_2, the ionization energies of CS and CO, and the electron affinities of CN, NO, and PO[30]) may require adjustment.

It should be noted that Shum and Benson[31] report an experimental barrier of 8.4 kJ mol^{-1} for methyl radical addition to the C-center of CH_2=S at 681−723 K, which corresponds to around 12.1 kJ mol^{-1} at 0 K. However, in their kinetic scheme, Shum and Benson exclude the possibility of S-addition on the basis of the lower stability of the resulting C-centered radical. In contrast, our present calculations suggest that the reported barrier may correspond, at least in part, to addition to the S-center. Hence, given the possible errors in the mechanistic scheme upon which the measured rate coefficient depends, coupled with the inherent uncertainties in experimental estimates of radical-addition barriers, this experimental barrier cannot be used to discriminate between the various high-level estimates. Nonetheless, it can be observed that, regardless of whether the experimental barrier corresponds to C- or S-addition, the barrier of 12.1 kJ mol^{-1} is higher than the barriers calculated with the CBS-type methods and it instead tends to favor the W1 and G3-type results.

TABLE 11: Effect of Level of Theory on the Heats of Formation (0 K, kJ mol^{-1}) of the Reactants and Products in the •CH_3 + CH_2═S System[a]

level of theory	•CH_3	CH_2═S	•CH_3 + CH_2═S	•CH_2SCH_3	CH_3CH_2S•
CBS-QB3//CC	152.4	118.9	271.3	152.3	115.3
CBS-RAD//CC	153.3	117.8	271.1	152.2	115.3
G3(MP2)-RAD//CC	147.3	115.6	262.9	151.4	112.0
G3X(MP2)-RAD//CC	147.7	115.1	262.8	150.6	112.2
G3-RAD//CC	149.2	121.2	270.4	156.0	114.3
G3X-RAD//CC	149.6	121.4	271.0	156.1	114.9
G3X(MP2)//CC	147.9	114.0	261.9	149.2	112.0
G3//CC	149.5	120.8	266.0	157.2	118.4
G3X//CC	147.4	118.8	266.2	152.8	114.3
W1//CC	148.5	122.8	271.3	148.0	112.9
experiment	150.0 ± 0.3[b]	118 ± 8.4[c]	268.0 ± 8.7	147.7 ± 5.9[d]	

[a] The notation //CC means that the composite methods are modified by replacing their prescribed geometries with CCSD(T)/6-311+G(d,p) geometries and their prescribed ZPVEs by QCISD/6-31G(d) ZPVEs scaled by a factor of 0.9776[23] (see text). [b] From ref 34. [c] From ref 33. [d] From ref 32.

For the reaction enthalpies, the trends are more complicated. While, as noted above, the difference between the CBS-type and W1 methods is slightly reduced (possibly because the influence of spin contamination diminishes), the errors in the G3-type methods actually increase, especially for the addition to S where even the best G3-type method shows a difference from W1 of 8.5 kJ mol^{-1}. In all cases, the other composite methods overestimate the reaction enthalpies for addition to both the C- and S-centers, compared with W1. They also overestimate the relative energy of the C-centered radical, compared with the S-centered radical. Of the G3-type methods, the "RAD" variants perform slightly better than their corresponding non-RAD versions, though some of the non-RAD methods outperform the RAD versions for the methyl-transfer enthalpies through cancellation of error. Within these modified G3-type methods (for which the geometry and ZPVE are calculated at a consistent level of theory), the simplification from G3X to G3 introduces minimal change (no more than 0.3 kJ mol^{-1}) but the "(MP2)" simplification can at times introduce a further error of 5−6 kJ mol^{-1}, though it is usually closer to 3 kJ mol^{-1}.

To understand further the behavior of the different methods, it is helpful to examine the heats of formation of the different stable species (see Table 11). Where experimental values are available,[32−34] the calculated heats of formation for all of the composite methods fall within the quoted experimental uncertainties, except in the case of the methyl radical for which the quoted experimental uncertainty is very small (0.3 kJ mol^{-1}). In this case the largest deviation in any of the composite methods is only 3.3 kJ mol^{-1}, and both W1 and the best G3-RAD methods have deviations less than 2 kJ mol^{-1}. The various composite methods are also in reasonable agreement with one another, with the maximum range for the various estimates of the heat of formation for a given species being approximately 8 kJ mol^{-1}. This maximum variation occurs for the C-centered radical, for which all of the composite methods give heats of formation that are larger than the W1 estimate (which is, however, well supported by the experimental value). In contrast, the various methods are in excellent agreement for the S-centered radical (for which the maximum variation in the alternative estimates of its heat of formation is just 3.4 kJ mol^{-1}). In general, while their performance is well within reasonable expectations, none of the less-expensive composite methods consistently provides very close agreement with the W1 values; however, the G3-RAD-type methods are probably the best overall performers when both the reaction enthalpies and heats of formation are considered.

For the methyl-transfer barriers (calculated relative to the energy of the S-centered radical), the various methods are in reasonable agreement, with the CBS-type methods again showing the largest deviation from W1, underestimating the reaction barriers by 3.8 kJ mol^{-1}. The majority of the G3-type methods have much smaller deviations, with the best G3-RAD estimate differing from W1 by less than 2 kJ mol^{-1}. The reverse barriers, of course, show greater variation because they are calculated from the energy of the C-centered radical, for which the various methods show greater variation. For the G3-RAD and CBS-type methods, the deviations increase slightly, while for the non-RAD variants of G3 the deviations decrease through cancellation.

In summary, it seems reasonable to suppose that the W1 method produces the best reaction barriers and enthalpies. The W1 calculations are reasonably well approximated by the less computationally expensive CBS- and G3-type methods. The "(MP2)" simplificatiion to the G3-type methods introduces an additional error of up to 6 kJ mol^{-1} to the absolute reaction enthalpies. However, the error is usually much smaller than this and these methods would thus be acceptable when the size of the system renders the cost of the full methods prohibitive. Of all the alternative methods, the "RAD" variants of G3 are the most consistent performers across the potential energy surface. However, even for these methods, deviations from W1 of up to 8 kJ mol^{-1} are found, especially when the C-centered radical is involved in the calculations. Fortunately, however, the agreement between the various composite methods is excellent for the relative barriers and enthalpies (within 2 kJ mol^{-1}, see Table 10). Hence reasonable approximations to the W1 barriers and enthalpies may be achieved using the W1 method for small model systems and, where W1 calculations cannot be afforded, using a simpler method such as G3(MP2)-RAD to measure the substituent effects. To this end, approximate W1 estimates for the various quantities in the methyl-substituted systems have been included in Tables 8 and 9. These were obtained by adding the G3(MP2)-RAD estimate of the substituent effect to the W1 estimate of the corresponding quantity in the unsubstituted system.

Standard Composite Methods. It is only feasible to perform high-level geometry optimizations and frequency calculations such as those employed above for relatively simple systems. It is therefore desirable to identify alternative levels at which to apply the composite methods. One possibility is to use the standard composite methods with their prescribed geometries and zero-point vibrational energies. The problem with this approach is, as noted above, that the majority of these composite methods prescribe B3-LYP methods for optimizing the geometries and calculating the zero-point vibrational energies and, as shown above, these methods are not suitable for optimizing

the transition structures in the addition reactions. This can be seen by comparing values (of the various enthalpies and barriers in Tables 7−9) obtained with the standard composite methods with those obtained with the corresponding high-level composite methods. Whereas the enthalpies for the methyl-radical-addition and -transfer reactions and the barriers for the methyl-transfer reactions obtained with the standard methods are in excellent agreement with their corresponding high-level counterparts (having errors of up to 2.7 kJ mol^{-1} but typically much less), the errors in the addition barriers obtained with the standard methods are considerably larger (up to 14.3 kJ mol^{-1}) when B3-LYP geometries are employed. The errors do diminish somewhat on methyl substitution, the dimethyl-substituted system having errors less than 6 kJ mol^{-1}; however, these additional errors are still unacceptably large, especially in the context of the small size of the reaction barriers in the present systems.

IRCmax Composite Methods. Fortunately, as shown above, the IRCmax technique of Petersson et al.[14] corrects for deficiencies in the B3-LYP addition transition structures. To demonstrate its success in approximating the high-level composite methods, IRCmax composite methods (obtained by applying the IRCmax procedure to the standard composite methods) were used to calculate improved barriers for methyl addition to the C- or S-centers of CH_2═S, and the results are included in Table 7. It is clear from these data that IRCmax barriers show excellent agreement with their corresponding high-level counterparts (with errors of less than 1 kJ mol^{-1}), and hence the IRCmax procedure offers an excellent substitute for the high-level optimizations.

In addition to the full IRCmax calculations, a new two-stage IRCmax procedure was also examined. As noted above, in a standard IRCmax calculation, high-level single points are calculated along a low-level IRC and the IRCmax transition structure is located as the maximum in the high-level reaction path, as plotted using the high-level single-points. In situations where multiple calculations using expensive composite methods cannot be afforded, an alternative approach is to identify the IRCmax transition structure using single points at an intermediate level of theory. The expensive composite method can then be applied as a traditional single-point calculation at the IRCmax transition structure. To test this two-stage IRCmax procedure, the IRCmax transition structures were obtained from CCSD(T)/6-311+G(d,p) single points (as these were available from the above geometry assessment) and barriers were calculated with the standard composite methods at these points. It is found that such barriers differ from the full IRCmax barriers by less than 0.5 kJ mol^{-1} and hence offer suitable substitutes to the full IRCmax procedure. Of course, this is merely a proof-of-principle test and specific further testing would be required if lower-level single-points were to be substituted for the CCSD(T) single-points.

Cheap Composite Methods. Since the IRCmax procedure requires the energy of the transition structure to be calculated at a number of points along the minimum energy path, this increases the cost and complexity of the calculation. It is therefore desirable to identify a low-cost alternative to IRCmax, that could be used for larger systems. To this end, cheap composite methods, in which the standard composite methods are employed with HF/6-31G(d) geometries and ZPVEs, are included in Tables 7−9. As noted in the geometry assessment, the HF/6-31G(d) level is found to provide excellent approximations to the high-level transition-structure geometries in the addition reactions, though it fares poorly for the methyl-transfer transition structures. These trends are reflected in the results in Tables 7−9. The cheap composite methods provide excellent approximations to their high-level counterparts for the addition barriers and for all of the reaction enthalpies (with errors of less than 2.5 kJ mol^{-1}, typically much less). However, as expected, they fail for the methyl-transfer barriers (with errors of up to 19.4 kJ mol^{-1}).

In summary, the standard composite methods may be used with their prescribed geometries and frequencies, provided that the addition barriers are improved using the IRCmax technique. When this cannot be afforded computationally, the use of HF/6-31G(d) geometries and frequencies provides an excellent substitute for the methyl-radical-addition reactions, though they are not suitable for the methyl-transfer reactions (for which the standard methods perform well).

Low-Level Methods. Thus far, the energy assessment has concentrated on the relative performance of a variety of standard and modified composite methods for the energy calculations. While some of these methods are less computationally expensive than others, the cost of all of these methods is prohibitive for larger systems. It is therefore desirable to identify which (if any) low-level methods can provide reasonable approximations to the high-level results. To this end, the barriers and enthalpies were also calculated using various low-level single-point energies and the results are included in Tables 7−9. Selected relative barriers and enthalpies showing the effects of methyl substitution are presented in Table 10. On the basis of these results, the following observations may be made.

The first observation concerns the choice of geometry. As noted above, the B3-LYP methods perform poorly for the methyl-radical-addition transition structures and the HF methods perform poorly for the methyl-transfer reactions. As expected, this is again the case when these geometries are used for the low-level single-point-energy calculations (see Tables 7−9). Hence the first conclusion that may be drawn is that, as for the high-level methods, the HF geometries and ZPVEs should not be used for the methyl-transfer reactions and B3-LYP methods should not be used for the methyl-radical-addition barriers.

The second observation that may be made is that, even when the appropriate geometries and ZPVEs are used, the DFT methods do not provide ideal low-cost approximations to the high-level methods. It is true that both the large-basis restricted and unrestricted B3-LYP single-points provide moderately good approximations to the W1 estimates for the same quantities in the unsubstituted system, in some cases having smaller errors than many of the high-level G3-type and CBS-type methods. However, when the substituted systems are considered, the errors in the RB3-LYP and UB3-LYP single-points increase substantially, particularly for reaction enthalpies. In the worst case, the error in the enthalpy for addition to the C-center increases from 10 kJ mol^{-1} to 24 kJ mol^{-1} and 35 kJ mol^{-1} for the monomethyl- and dimethyl-substituted systems, respectively. Put another way, these methods do not adequately describe the effect of methyl substitution on the relative barriers and enthalpies, having errors greater than 10 kJ mol^{-1} in the relative quantities for the monosubstituted system and up to 25 kJ mol^{-1} in the disubstituted system (see Table 10). The performance of the small-basis B3-LYP single-points is even worse, with this method having errors of more than 10 kJ mol^{-1}, even in the unsubstituted system. Likewise, the density functional method MPW1K is not a suitable low-cost alternative to the high-level methods. While it provides absolute reaction barriers for the addition reactions that fall within the range of values spanned by the various high-level composite methods, the errors in the reaction enthalpies and the methyl-transfer barriers are very large

TABLE 12: Best Estimates of Barriers and Enthalpies (0 K, kJ mol^{-1}) for Methyl-Radical-Addition and Methyl-Transfer Reactions in the ·CH$_3$ + CXY═S System (for X, Y = H or CH$_3$)[a]

	add to C		add to S		C• → S•	
system	ΔH	$\Delta H^{\ddagger}$	ΔH	$\Delta H^{\ddagger}$	ΔH	$\Delta H^{\ddagger}$
·CH$_3$ + CH$_2$═S	−158.5	13.7	−123.4	8.2	−35.1	204.6
·CH$_3$ + CH$_3$CH═S	−142.0	19.7	−106.5	9.8	−35.5	191.4
·CH$_3$ + C(CH$_3$)$_2$═S	−132.7	25.8	−94.0	10.7	−38.7	178.3

[a] Corresponding to the W1 level of theory for the unsubstituted system and the "approximate W1" level of theory for the substituted systems (see text).

(over 20 kJ mol^{-1} in the unsubstituted system). More importantly, perhaps, the errors in all of the relative barriers and enthalpies are comparable to those of the large-basis B3-LYP single-points (see Table 10) and are thus unacceptably high.

The final observation is that the use of RMP2 single-points with a large basis set does offer a promising low-cost alternative to the high-level methods. Provided that HF geometries are used for the methyl-radical-addition transition structures and B3-LYP geometries are used for the methyl-transfer transition structures, the large-basis RMP2 single-point calculations provide barriers and enthalpies that fall within 10 kJ mol^{-1} of the high-level results for all of the reactions in the unsubstituted system (see Table 7). Even more promising is the observation that the errors in the various *relative* quantities are approximately 2 kJ mol^{-1} for the monosubstituted system and around 4 kJ mol^{-1} for the di-substituted system (see Table 10). Hence this technique might be suitable when the high-level methods cannot be afforded, especially if only relative barriers and enthalpies are required.

D. Addition to C═S Bonds: Does Kinetics Follow Thermodynamics? Having identified suitable levels of theory at which to calculate accurate reaction barriers and enthalpies, it is now possible to examine in more detail their values with a view to establishing whether addition should occur at the carbon or sulfur centers. To assist in the comparison of the results, the W1 (or "approximate W1", see above for details) barriers and enthalpies for all of the systems are collected in Table 12. From these data, a number of important observations may be made.

First, the results in Table 12 confirm the observations from earlier studies[4,5] that the S-centered radical arising from radical addition to the C-center of a C═S double bond is substantially more stable (by almost 40 kJ mol^{-1}) than the corresponding C-centered radical. The effect of methyl substitution at the C-center of the C═S bond is to decrease the exothermicity of both of the alternative addition reactions by similar amounts, with the relative stabilities of the resulting S- and C-centered radicals remaining reasonably unchanged.

The second point to emerge is confirmation that the addition reaction is contra-thermodynamic. That is, despite the clear thermodynamic preference for the S-centered radical product, the barriers for addition at the S-center are lower than those for addition at the C-center and hence it is the C-centered radical that should be obtained. While, especially for the unsubstituted system, the barriers for S- and C-addition are close, their difference does exceed the estimated uncertainty in the relative barriers and the result should thus be regarded as significant. The effect of methyl substitution is to increase the addition barriers at both centers, but particularly at the C-center, thus enhancing the preference for addition at the S-center. The relative C- and S-addition barriers increase from 5.5 kJ mol^{-1} to 9.9 kJ mol^{-1} and 15.1 kJ mol^{-1} for the monomethyl- and dimethyl-substituted systems, respectively. The contribution of the activation energy to the difference in C- and S-addition rates at room temperature is thus approximately 1, 2, and 3 orders of magnitude for the unsubstituted, monomethyl and dimethyl systems, respectively. While we have not yet calculated the overall rate coefficients for the alternative addition reactions, it seems reasonable to suppose that the entropic factors would also favor addition to the S-center of the C═S bond as this is less crowded, especially in the methyl-substituted cases.

A third point is that the results for the methyl-transfer reaction reveal that the transfer barrier is very high (up to 205 kJ mol^{-1} above the C-centered radical, and up to 85 kJ mol^{-1} above the isolated reactants), and hence this does not provide an alternative pathway for interconversion between the kinetically favored but less-stable C-centered radical and the more-stable S-centered radical. The effect of methyl substitution is to reduce the transfer barrier (as measured from the C-centered radical) slightly, through the relative destabilization of the reactant (and product) radicals compared with the transition structure (which remains at around 85 kJ mol^{-1} above the isolated reactants). However, even in the dimethyl-substituted system, the transfer barrier exceeds the energy required for fragmentation to a methyl radical plus the thiocarbonyl, followed by re-addition of the methyl radical to the C-center. Hence the methyl-transfer barrier remains far too high for this to be a viable pathway for the conversion of C-centered to S-centered radicals. In summary, the present work confirms that radical addition to C═S bonds is contra-thermodynamic (at least for the present systems) and supports the recent speculation by Carmichael et al.[4] that this preference for addition to the S-center is the result of kinetic factors.

The results in Table 12 also have interesting implications for practical applications involving radical addition to C═S bonds. One important application of radical addition to C═S bonds is the reversible-addition-fragmentation-transfer ("RAFT") process for control of molecular weight and architecture in free-radical polymerization.[1] This process relies on addition of the initiator or growing polymer radical to the S-center of the C═S bond in thiocarbonyl compounds (typically of the form S═C(Z)SR), followed by fragmentation of one or other of the two S−C bonds in order to re-form a thiocarbonyl compound and a C-centered radical. While the results in Table 12 support the assumption inherent in the RAFT process that the addition occurs at the S-center rather than the C-center, they also suggest that there may be substituents for which this may not necessarily be the case. For instance, in the unsubstituted system in Table 12, the difference between the barriers for addition to S and C is very small (just 5.5 kJ mol^{-1}). Because this difference corresponds to a difference in reaction rates of just 1 order of magnitude at room temperature, one might expect that some of the C-addition product would form in this case. It would therefore not be surprising for the C-addition reaction to be a significant side-reaction for appropriately substituted thiocarbonyl compounds, and this may be a useful point of inquiry when, for specific thiocarbonyl compounds, the RAFT process is found to be unsuccessful.

A second observation from Table 12 is that radical addition to C═S bonds (whether to the S- or the C-center) is highly exothermic and hence the reverse barrier (for fragmentation) would generally be expected to be quite high. This not only supports earlier observations that thiocarbonyl agents could make good radical traps,[35] but also provides circumstantial support for recent controversial claims that the thiocarbonyl compound cumyl dithiobenzoate[36] (for which the substituent Z in S═C(Z)SR is a highly stabilizing phenyl group) produces

TABLE 13: Effect of Level of Theory on the Barriers and Enthalpies (0 K, kJ mol^{-1}) for Rotation about the ·C−S Bond in ·CXYSCH$_3$ (X, Y = H or CH$_3$) Radicals[a]

	X, Y = H, H		X, Y = H, CH$_3$		X, Y = CH$_3$, CH$_3$	
level of theory	ΔH	$\Delta H^{\ddagger}$	ΔH	$\Delta H^{\ddagger}$	ΔH	$\Delta H^{\ddagger}$
Low-Level Methods						
B3-LYP/6-31G(d)//HF	0.0	23.0	3.5	15.8	0.0	10.4
B3-LYP/6-311+G(3df,2p)//HF	0.0	30.3	4.4	20.6	0.0	13.4
RB3-LYP/6-311+G(3df,2p)//HF	0.0	30.2	4.4	20.7	0.0	13.4
RMP2/6-311+G(3df,2p)//HF	0.0	26.0	3.8	18.6	0.0	12.8
B3-LYP/6-31G(d)//B3	0.0	23.2	3.5	15.7	0.0	9.6
B3-LYP/6-311+G(3df,2p)//B3	0.0	31.2	4.3	21.2	0.0	13.0
RB3-LYP/6-311+G(3df,2p)//B3	0.0	30.8	4.3	21.3	0.0	13.1
RMP2/6-311+G(3df,2p)//B3	0.0	28.5	3.5	20.2	0.0	13.8
MPW1K/6-31+G(d,p)//MPW1	0.0	24.5	3.9	15.8	0.0	9.7
MPW1K/6-311+G(3df,2p)//MPW2	0.0	29.3	4.4	19.6	0.0	12.1
Cheap Composite Methods						
CBS-RAD//HF	0.0	28.4	4.6	22.0	0.0	16.5
G3(MP2)-RAD//HF	0.0	26.5	3.3	18.2	0.0	12.7
G3X//HF	0.0	27.3	3.4	18.9	0.0	13.3
Standard Composite Methods						
CBS-QB3	0.0	30.5	3.4	20.9	0.0	14.1
CBS-RAD (B3,B3)	0.0	29.9	4.1	23.1	0.0	17.4
G3(MP2)-RAD	0.0	28.1	3.2	19.6	0.0	13.2
G3X	0.0	29.6	3.4	20.7	0.0	13.9
High-Level Composite Methods						
CBS-RAD//QCI	0.0	30.4[b]	4.1	22.9	0.0	17.0
G3(MP2)-RAD//QCI	0.0	28.5[b]	3.0	19.2	0.0	12.9
G3X//QCI	0.0	29.4[b]	3.0	19.9	0.0	13.5
W1//QCI	0.0	30.6[b]	3.0[c]	21.3[c]	0.0	15.0[c]

[a] See footnote *a* from Table 7. [b] Calculated with CCSD(T)/6-311+G(d,p) geometries. [c] Approximate W1 values, as described in the text.

highly stable, long-lived radicals in the RAFT process. Further studies along these lines are in progress.[37]

E. Barriers for Rotation about the ·C−S Bond. Since two stable conformers of the ·CH(CH$_3$)SCH$_3$ radical are found (structures **8** and **9** in Figure 3), it is of interest to explore the rotational barriers about the ·C−S bond for this radical and for ·CH$_2$SCH$_3$ (**7**) and ·C(CH$_3$)$_2$SCH$_3$ (**10**). These were calculated at a variety of moderate to very high levels of theory and are shown in Table 13. The first observation that can be made concerning these data is that the rotational barriers and enthalpies are relatively insensitive to the level of theory and, with the exception of the small-basis-set B3-LYP and MPW1K energies, all of the methods are in reasonable agreement. This is not surprising since we are merely comparing the relative energies of different conformations of the same radical and hence we would expect significant cancellation of error. In the unsubstituted system, the rotational barrier is approximately 30 kJ mol^{-1}, much larger than the corresponding barrier for the rotation about the ·C−O bond in the ·CH$_2$OCH$_3$ radical (which is 20 kJ mol^{-1} at the CBS-RAD level).[38] The size of the rotational barrier might be expected to reflect the strength of the stabilizing interaction between the unpaired electron at the radical center and the p-type lone pair on the heteroatom in the stable radical species (since this stabilizing influence is possible in the stable conformers but not in the (orthogonal) rotational transition structures). Hence, the larger rotational barrier for the ·C−S bond in the ·CH$_2$SCH$_3$ radical suggests that the stabilizing interaction with the sulfur lone pair in the ·CH$_2$SCH$_3$ radical is stronger than with the oxygen lone pair in the ·CH$_2$OCH$_3$ radical. While this might seem surprising, it is to some extent supported by the earlier observation that the radical stabilization energy of the ·CH$_2$SH radical is larger than that of the ·CH$_2$OH radical.[39] On methyl substitution, the ·C−S rotational barrier in the ·CXYSCH$_3$ radical decreases substantially to approximately 21 kJ mol^{-1} for the mono- and approximately 15 kJ mol^{-1} for the di-substituted systems. This perhaps reflects the hyperconjugative stabilizing effect of the methyl substituents in the rotational transition structure.

4. Conclusions

In this study we have performed an extensive assessment of theoretical procedures for calculating the geometries, zero-point vibrational energies, and electronic energies for the reactants, products, and transition structures in the addition of the methyl radical to prototypical thiocarbonyl compounds, and for the methyl-transfer reaction that interconverts the C- and S-centered radical products. Our main conclusions from this assessment are as follows.

(1) Geometry optimizations and zero-point vibrational energy (ZPVE) calculations are generally relatively insensitive to the level of theory. However, HF methods are not suitable for the methyl-transfer transition structures, and B3-LYP methods are not suitable for the methyl-radical-addition transition structures. Therefore, the standard composite methods that use B3-LYP geometries and ZPVEs are not suitable for studying the methyl-radical-addition barriers. This highlights the need for caution when applying these high-level composite methods as they may sometimes be compromised by the DFT methods prescribed for the geometry optimizations. In the present case, this problem can be overcome using higher-level geometry optimizations and ZPVE calculations, or using an IRCmax procedure to further optimize the B3-LYP transition structures. In the latter case, the B3-LYP ZPVE calculations should be carried out on the IRCmax transition structures. The use of HF methods for the geometry optimizations and ZPVE calculations provides an adequate lower-cost alternative to these measures. The density functional method MPW1K was also explored as an alternative to the B3-LYP methods for the addition-transition-structure geometry optimizations. While it is found to offer

marginal improvements to the small-basis B3-LYP geometries, and is comparable in performance to the large basis B3-LYP methods, its performance is not as good as the lower-cost HF methods.

(2) Even with high-level geometries and ZPVEs, there is some disagreement among the different classes of composite methods for *absolute* reaction barriers and enthalpies in the addition and transfer reactions. Assuming that the highest-level method examined, W1, is the most accurate, the G3-RAD-type methods are perhaps the best lower-cost alternative to W1, though even these methods show deviations of up to 8 kJ mol^{-1} from W1 in the calculations involving the C-centered radical product.

(3) The various composite methods do show good agreement in the *relative* barriers and enthalpies, both with respect to methyl substitution and on comparison of S- and C-addition barriers. Hence, a low-cost alternative to the high-level W1 calculations is to calculate the absolute quantities via W1 on the simplest model system and add to this the substituent effect, as calculated with a lower-level method such as G3-(MP2)-RAD.

(4) Restricted or unrestricted B3-LYP single-points with a large basis set (on either HF or B3-LYP geometries) and large- or small-basis MPW1K energies (on MPW1K geometries) do not provide a suitable low-cost method for studying these reactions, as these methods show very large errors in both the absolute and relative enthalpies for many of the methyl-radical-addition and -transfer reactions studied.

(5) The use of RMP2/6-311+G(3df,2p) single-point energies, calculated on B3-LYP/6-31G(d) geometries for the methyl-transfer reactions and HF/6-31G(d) geometries for the addition reactions, together with appropriate ZPVE corrections, provides a reasonable low-cost method for larger systems. This method has errors of around 10 kJ mol^{-1} in absolute barriers and enthalpies and up to 4 kJ mol^{-1} in the relative quantities.

We have also examined whether methyl radical addition to thiocarbonyl compounds would be expected to occur predominantly at the C- or S-centers of the C═S bond. We find that for thioformaldehyde, and its mono- and dimethyl-substituted derivatives, addition at the S-center should occur because of a lower calculated barrier, despite a clear thermodynamic preference for the S-centered radical product arising from addition at the C-center of the C═S bond. Furthermore, we find that the methyl-transfer reaction that interconverts these two radicals does not provide a low-energy pathway for obtaining the more stable radical. Hence the less stable, C-centered radical should be the major product and the reaction is contra-thermodynamic. We also find that methyl radical addition to both centers is highly exothermic, though this exothermicity decreases somewhat on methyl substitution. The methyl substituents do not substantially alter the relative stabilities of the C- and S-centered radicals but do increase the reaction barriers for addition to both centers and also the relative preference for addition at the S-center. These results have interesting implications for the RAFT process in free-radical polymerization, and further studies in this direction are currently in progress.[37]

Acknowledgment. We gratefully acknowledge generous allocations of computing time on the Compaq Alphaserver of the National Facility of the Australian Partnership for Advanced Computing and the Australian National University Supercomputing Facility, provision of an Australian Research Council postdoctoral fellowship (to M.L.C.) and an Australian National University Summer Research Scholarship (to G.P.F.W.), and useful discussions with Dr David Henry.

Supporting Information Available: Table S1 contains GAUSSIAN archive entries for the QCISD/6-31G(d) geometries of all species studied in the present work. This material is available free of charge via the Internet at http://pubs.acs.org.

References and Notes

(1) Chiefari, J.; Chong, Y. K. B.; Ercole, F.; Krstina, J.; Jeffery, J.; Le, T. P. T.; Mayadunne, R. T. A.; Meijs, G. F.; Moad, C. L.; Moad, G.; Rizzardo, E.; Thang, S. H. *Macromolecules* **1998**, *31*, 5559.

(2) Destarac, M.; Charmot, D.; Franck, X.; Zard, S. Z. *Macromol. Rapid Commun.* **2000**, *21*, 1035.

(3) For detailed reviews of the radical chemistry associated with the thiocarbonyl group, see for example: (a) Crich, D.; Quintero, L. *Chem. Rev.* **1989**, *89*, 1413. (b) Zard, S. Z. *Angew. Chem., Int. Ed. Engl.* **1997**, *36*, 672.

(4) Macrae, R. M.; Carmichael, I. *J. Phys. Chem. A* **2001**, *105*, 3641.

(5) Chiu, S. W.; Cheung, Y.-S.; Ma, N. L.; Li, W.-K.; Ng, C. Y. *J. Mol. Struct. THEOCHEM* **1997**, *397*, 87.

(6) Curtiss, L. A.; Raghavachari, K.; Trucks, G. W.; Pople, J. A. *J. Chem. Phys.* **1991**, *94*, 7221.

(7) Hehre, W. J.; Radom, L.; Schleyer, P. v. R.; Pople, J. A. *Ab Initio Molecular Orbital Theory*; Wiley: New York, 1986.

(8) Koch, W.; Holthausen, M. C. *A Chemist's Guide to Density Functional Theory*; Wiley-VCH: Weinheim, 2000.

(9) Frisch, M. J.; Trucks, G. W.; Schlegel, H. B.; Scuseria, G. E.; Robb, M. A.; Cheeseman, J. R.; Zakrzewski, V. G.; Montgomery, J. A., Jr.; Stratmann, R. E.; Burant, J. C.; Dapprich, S.; Millam, J. M.; Daniels, A. D.; Kudin, K. N.; Strain, M. C.; Farkas, O.; Tomasi, J.; Barone, V.; Cossi, M.; Cammi, R.; Mennucci, B.; Pomelli, C.; Adamo, C.; Clifford, S.; Ochterski, J.; Petersson, G. A.; Ayala, P. Y.; Cui, Q.; Morokuma, K.; Malick, D. K.; Rabuck, A. D.; Raghavachari, K.; Foresman, J. B.; Cioslowski, J.; Ortiz, J. V.; Stefanov, B. B.; Liu, G.; Liashenko, A.; Piskorz, P.; Komaromi, I.; Gomperts, R.; Martin, R. L.; Fox, D. J.; Keith, T.; Al-Laham, M. A.; Peng, C. Y.; Nanayakkara, A.; Challacombe, M.; Gill, P. M. W.; Johnson, B.; Chen, W.; Wong, M. W.; Andres, J. L.; Gonzalez, C.; Head-Gordon, M.; Replogle, E. S.; Pople, J. A. *GAUSSIAN 98*; Gaussian, Inc.: Pittsburgh, PA, 1998.

(10) Werner, H.-J.; Knowles, P. J.; Amos, R. D.; Bernhardsson, A.; Berning, A.; Celani, P.; Cooper, D. L.; Deegan, M. J. O.; Dobbyn, A. J.; Eckert, F.; Hampel, C.; Hetzer, G.; Korona, T.; Lindh, R.; Lloyd, A. W.; McNicholas, S. J.; Manby, F. R.; Meyer, W.; Mura, M. E.; Nicklass, A.; Palmieri, P.; Pitzer, R.; Rauhut, G.; Schütz, M.; Stoll, H.; Stone, A. J.; Tarroni, R.; Thorsteinsson, T. MOLPRO 2000.6; University of Birmingham: Birmingham, 1999.

(11) Stanton, J. F.; Gauss, J.; Watts, J. D.; Nooijen, M.; Oliphant, N.; Perera, S. A.; Szalay, P. G.; Lauderdale, W. J.; Kucharski, S. A.; Gwaltney, S. R.; Beck, S.; Balková, A.; Bernholdt, D. E.; Baeck, K. K.; Rozyczko, P.; Sekino, H.; Hober, C.; Bartlett, R. J. ACES II; Quantum Theory Project, University of Florida: Gainsville, 1992.

(12) Curtiss, L. A.; Raghavachari, K.; Redfern, P. C.; Rassolov, V.; Pople, J. A. *J. Chem. Phys.* **1998**, *109*, 7764.

(13) Martin, J. M. L.; De Oliveira, G. J. *J. Chem. Phys.* **1999**, *111*, 1843.

(14) Malick, D. K.; Petersson, G. A.; Montgomery, J. A. *J. Chem. Phys.* **1998**, *108*, 5704.

(15) Baboul, A. G.; Schlegel, H. B. *J. Chem. Phys.* **1997**, *107*, 9413.

(16) Curtiss, L. A.; Redfern, P. C.; Raghavachari, K.; Rassolov, V.; Pople, J. A. *J. Chem. Phys.* **1999**, *110*, 4703.

(17) Baboul, A. G.; Curtiss, L. A.; Redfern, P. C.; Raghavachari, K. *J. Chem. Phys.* **1999**, *110*, 7650.

(18) Curtiss, L. A.; Redfern, P. C.; Raghavachari, K.; Pople, J. A. *J. Chem. Phys.* **2001**, *114*, 108.

(19) Henry, D. J.; Parkinson, C. J.; Radom, L. *J. Phys. Chem. A* **2002**, *106*, 7927.

(20) Montgomery, J. A., Jr.; Frisch, M. J.; Ochterski, J. W.; Petersson, G. A. *J. Chem. Phys.* **1999**, *110*, 2822.

(21) Mayer, P. M.; Parkinson, C. J.; Smith, D. M.; Radom, L. *J. Chem. Phys.* **1998**, *108*, 604.

(22) Parthiban, S.; Martin, J. M. L. *J. Chem. Phys.* **2001**, *114*, 6014.

(23) Scott, A. P.; Radom, L. *J. Phys. Chem.* **1996**, *100*, 16502.

(24) Lynch, B. J.; Truhlar, D. G. *J. Phys. Chem. A* **2001**, *105*, 2936.

(25) Lynch, B. J.; Fast, P. L.; Harris, M.; Truhlar, D. G. *J. Phys. Chem. A* **2000**, *104*, 4811.

(26) Lias, S. G.; Bartmess, J. E.; Liebman, J. F.; Holmes, J. L.; Levin, R. D.; Mallard, W. G. *J. Phys. Chem. Ref. Data* **1988**, *17, Supplement No. 1*.

(27) Nicolaides, A.; Rauk, A.; Glukhovtsev, M. N.; Radom, L. *J. Phys. Chem.* **1996**, *100*, 17460.

(28) Wong, M. W.; Radom, L. *J. Phys. Chem.* **1995**, *99*, 8582.

(29) This is also known as the CBSB3 basis set and consists of the 6-311+G basis set with the addition of three d-type and one f-type polarization functions on all second-row atoms, two d-type and one f-type polarization functions on all first-row atoms, and two p-type polarization functions on all hydrogen atoms.

(30) Ochterski, J. W.; Petersson, G. A.; Montgomery, J. A. *J. Chem. Phys.* **1996**, *104*, 2598.

(31) Shum, L. G. S.; Benson, S. W. *Int. J. Chem. Kinet.* **1985**, *17*, 749.

(32) Jefferson, A.; Nicovich, J. M.; Wine, P. H. *J. Phys. Chem.* **1994**, *98*, 7128.

(33) Ruscic, B.; Berkowitz, J. *J. Chem. Phys.* **1993**, *98*, 2568.

(34) Ruscic, B.; Litorja, M.; Asher, R. L. *J. Phys. Chem. A* **1999**, *103*, 8625.

(35) Tsuchihashi, G.; Yamauchi, M.; Ohno, A. *Bull. Chem. Soc. Jpn.* **1970**, *43*, 968.

(36) Barner-Kowollik, C.; Vana, P.; Quinn, J. F.; Davis, T. P. *J. Polym. Sci., Part A: Polym. Chem.* **2002**, *40*, 1058.

(37) Coote, M. L.; Radom, L. *J. Am. Chem. Soc.*, submitted.

(38) Henry, D. J.; Beckwith, A. L. J.; Radom, L. To be published.

(39) Henry, D. J.; Parkinson, C. J.; Mayer, P. M.; Radom, L. *J. Phys. Chem. A* **2001**, *105*, 6750.